Study of the interaction of a solitary wave with a submerged obstacle through a depth semi-averaged model

G. Colicchio[1,2] **M. Antuono**[1]
giuseppina.colicchio@cnr.it **matteo.antuono@cnr.it**

1 **CNR-INM, Institute of Marine Engineering, Rome, Italy.**
2 **AMOS, Marine Technology Department, NTNU, Trondheim, Norway.**

Ocean wave forecast and hindcast are very important in several fields linked to the exploitation of the coastlines. They are important for the construction and management of offshore structures and harbors and for naval operations. For example, in the case of harsh see conditions, it is important to understand the interaction of the waves and currents with the local bathymetry to guide the docking operations of vessels. Moreover, nowadays, to maximize the energy extraction of recent wave energy converters (WEC), the settings of the Power Take Off and the activation of the survival modes rely on the correct evaluation of the most energetic sites and on accurate and reliable wave forecasts.

While numerical ocean modeling forecast have been available for many years [4], it is only recently that the numerical models have been specialized for the forecast in more confined areas and the reliability of the models is still low compared to the required standard to maximize the energy extraction times for WECs.

Here, we use a non-hydrostatic model [2] that is efficiently able to follow the non-linear wave propagation while retaining the dispersion, shoaling, refraction, and diffraction features from deep to shallow water conditions. It overcomes some limitations of the commercial software like MIKE 3 [3]; in fact, the domain can assume whatever shape, with stretching in each of the coordinate direction to accommodate the local bathymetry and there is no limit in the direction of the inflow conditions.

It will be compared to a full 3D Navier-Stokes simulation for the interaction of a solitary wave with a submerged barrier in a narrow channel. A sketch of the problem is described in figure 1. A solitary wave enters a narrow channel with width $W = 16m$, depth $d = 1m$ and length $L = 24m$. A submerged obstacle is at the center of the channel. It is characterized by a rounded truncated pyramidal shape with lower base 10.64m x 6.55m and an upper base 6.94m x 0.9m, the height of the obstacle is 0.8m.

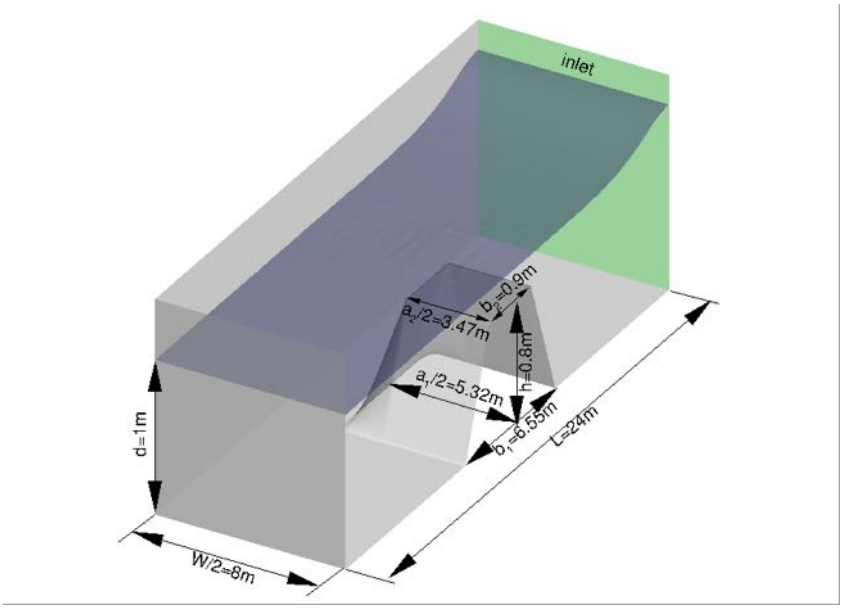

Figure 1: Sketch of the analyzed problem; the grey surfaces represent solid walls, the blue shade represents the free surface, the green region is the inlet area.

Description of the depth semi averaged model (DSAM) The Depth semi averaged model is well documented in [1], here, only the main features of the models are detailed for a case without wave breaking or friction along solid walls. Mass and momentum conservation of the flow are written as

$$d_t + \nabla \mathbf{Q} = 0 \tag{1}$$

$$\mathbf{M_t} + \nabla \cdot \mathcal{F} = (gd + p_b)\nabla h \tag{2}$$

where d is the vertical distance between the free surface η and the local bathymetry $(-h)$; $\mathbf{Q}$ is the mass flux vector; $\mathbf{U}$ is the depth-averaged velocity in the horizontal plane; $\mathbf{M}$ is the generalized mass flux and it is obtained as $\mathbf{M} = \mathbf{Q} + \int_{-h}^{\eta} \nabla \Gamma dz$, with Γ the semi-averaged vertical velocity component written as $\Gamma = \int_{-h}^{\eta} w dz$, w is the vertical component of the velocity, $p_b = \nabla \cdot \int_{-h}^{\eta} w\mathbf{u} dz$ is the dynamic pressure component at the seabed and $\mathbf{u}$ is horizontal velocity field. The flux term $\mathcal{F}$ takes into account the other dispersive contributions and the classic shallow-water terms,

$$\mathcal{F} = \left(g\frac{d^2}{2} + Disp \right) \mathcal{I} + \left(d\mathbf{U} \otimes \mathbf{U} + \int_{-h}^{\eta} (\delta\mathbf{u} \otimes \delta\mathbf{u}) dz \right) \tag{3}$$

where $\otimes$ is the dyadic product and $\delta\mathbf{u}$ represents the deviation of $\mathbf{u}$ with respect to the depth-averaged field $\mathbf{U}$, $\delta\mathbf{u} = -\nabla\Gamma + 1/d \int_{-h}^{\eta} \nabla\Gamma dz$. The non-linear dispersive term is

$$Disp = \nabla \cdot \left(\int_{-h}^{\eta} \int_{z}^{\eta} w\mathbf{u} d\xi \right) - \int_{-h}^{\eta} (w + \mathbf{u} \cdot \nabla h) dz. \tag{4}$$

The integrated continuity equation

$$\nabla^2 \Gamma = \nabla \cdot \left(\frac{\mathbf{M}}{d} \right) \tag{5}$$

gives the closer for Γ. Equations 1 and 2 are discretized using a fourth-order finite-volume discretization based on an HLL-MUSCL-Hancock scheme and a fourth-order Adams-Bashforth-Moulton predictor/corrector algorithm for the time integration, while equation 5 is approximated with a second-order finite-difference discretization.

Navier Stokes solver OpenFOAM is used for the Navier Stokes simulations of the problem in figure 1. A second order finite volume discretization is used in space and a second order implicit time marching scheme is used for the time evolution. The Volume of Fluid method is used to track the position of the free surface. Because using analytical conditions on the inlet boundary would cause oscillation downstream of the wave, a piston wave maker is used to initiate the wave.

Validation of the DSAM versus OpenFOAM A solitary wave with amplitude $a = 0.2m$ is used to validate the DSAM code. Here we underline that the spatial discretization of the DSAM is much coarser with the respect to the one used in the NS simulation; in x and y it is three time coarser and in the vertical direction z it is six times coarser above the obstacle. Practically, $\Delta x_{DSAM} = \Delta y_{DSAM} = 0.2m$, $\Delta y_{DSAM} = 0.05m$ are the dimension of the uniform Cartesian mesh that has been used in the DSAM simulations. In the NS simulation, the mesh is initially uniform in x and y but it stretches in the x direction to follow the motion of the wavemaker, later. In the vertical direction, the NS mesh is stretched around the undisturbed free surface.

Figure 2 shows the evolution of the wave as it overcomes the submerged obstacle. In each panel the position of the obstacle is plotted using the white solid lines and the upper part of the figure refers to the DSAM solution, the bottom part to the full 3D NS solution. Even though the generated waves have small differences (fig.2.a), the two solvers show a very similar behavior of the wave. There is a steeping of the wave as it approaches the obstacle (fig.2.b); while rising on the obstacle, the wave front curves, with a slower central part (fig.2.c and 2.d); some part of the wave is reflected back by the obstacle (light blue part in fig.2.e). While approaching the front edge of the obstacle, the wave

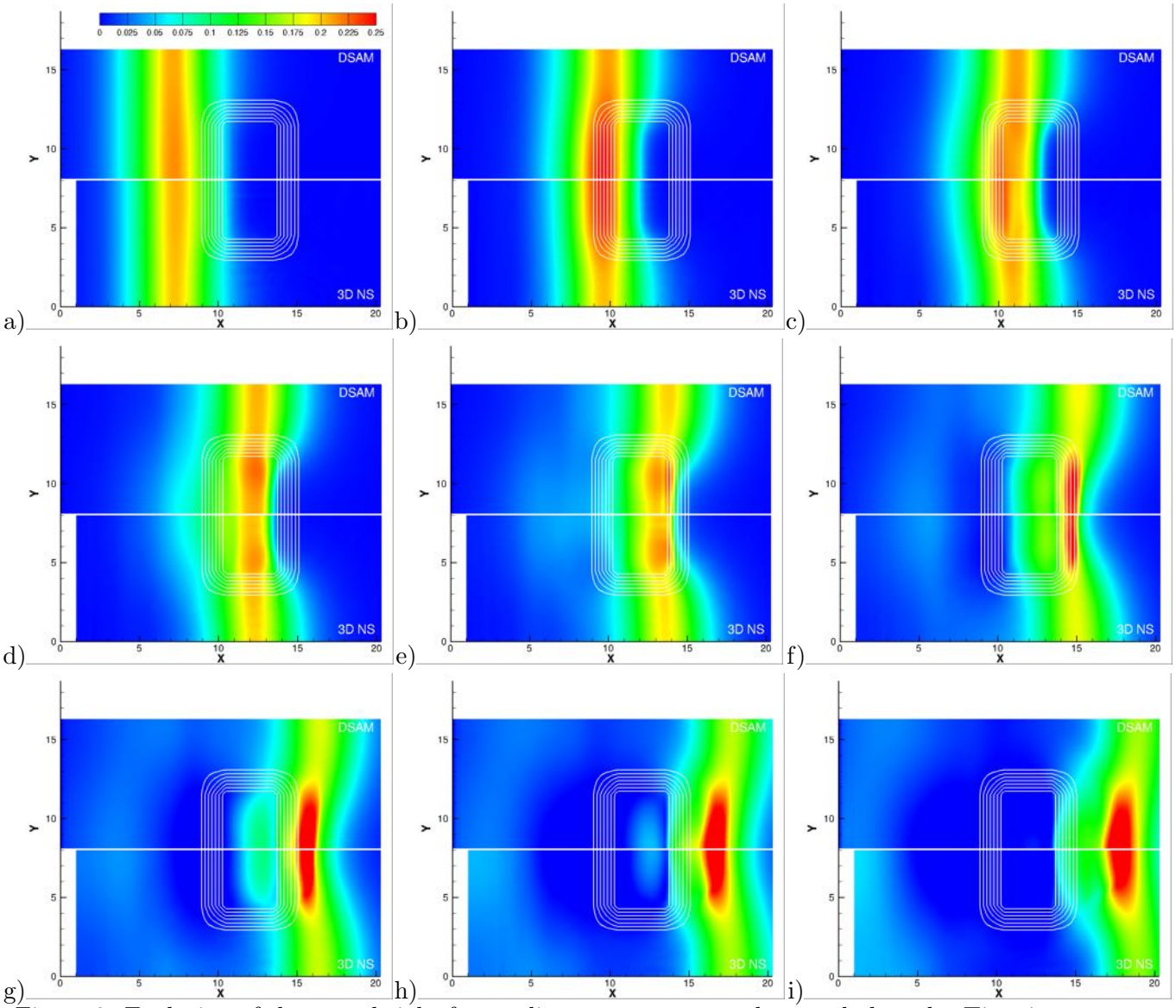

Figure 2: Evolution of the wave height for a solitary wave over a submerged obstacle. Time increases from one panel to the other with a $\Delta t = 0.4s$.

front steepens further (fig.2.f) and interacts with the front corner of the obstacle generating a sort of dent in the downstream side of the wave (fig.2.g). While flowing away from the obstacle, the wave front speeds up and forms a spilling breaker in the 3D NS solution (fig.2.h and fig.2.i).

Given the difference in the mesh resolution (200 thousand points in the DSAM versus 7 million points in the NS), the agreement in wave elevation is very good.

The largest errors are related to the dents that form on the free surface in correspondence with the upper edges of the barrier. Figure 3.a shows the 3D view of the wave height at the same time of figure 2.e. The dent in the front part of the wave is more emphasized by the DSAM, while the dent in the back is more evident in the 3D NS solution.

We have found that this error could be related to the diffused boundary method that is used to solve the Poisson equation 5; i.e. the distances from the free surface and from the body are used to smooth the Dirichlet condition on the free surface and the Neumann condition on the solid boundaries.

For the same time instant of figure 3.a, the Poisson equation has been solved using both the diffused boundary method and a new "cut cell" method to prescribe the boundary conditions in their exact position. The resulting vertical velocity on the $z = 0$ plane are plotted in fig.3.b and fig3.c

a) 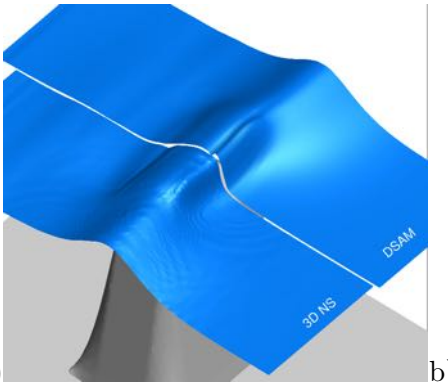

b) 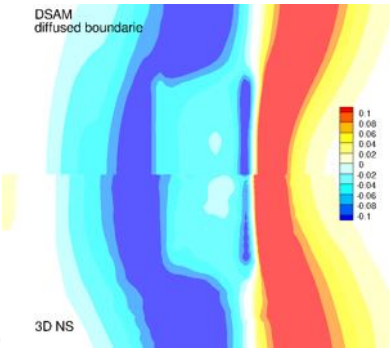

c) 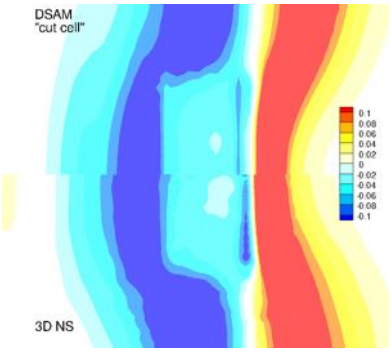

Figure 3: a) 3D view of the wave height of fig.2.e; b) comparison between the vertical velocity contours calculated using DSAM with diffused boundary (top) and using OpenFOAM (bottom); c) comparison between the vertical velocity calculated using DSAM with a "cut cell" method (top) and using OpenFOAM (bottom).

and compared with the velocity at the same height in the 3D NS solution. The diffused boundary method generates a more intense negative vertical velocity in correspondence with the front edge of the obstacle and a velocity less intense on the back side; while the "cut cell" method results resembles more closely those obtained with OpenFOAM.

These comparisons are promising. So the "cut cell" method will be used for the whole time simulation and the results will be presented at workshop to show that even such small discrepancies can disappear without any need to increase the mesh resolution and consequently the computational time.

Acknowledgment This research was developed within and supported by the MIUR PRIN 2017 Project "FUNdamentals of BREAKing wave-induced boundary dynamics - FUNBREAK", with grant number 20172B7MY9.

References

[1] M. Antuono, G. Colicchio, C. Lugni, M. Greco, and M. Brocchini. A depth semi-averaged model for coastal dynamics. *Physics of Fluids*, 29(5):056603, 2017.

[2] M. Antuono, S. Valenza, C. Lugni, and G. Colicchio. Validation of a three-dimensional depth-semi-averaged model. *Physics of Fluids*, 31(2):026601, 2019.

[3] DHI. Mike 3 flow model, user guide. *https://manuals.mikepoweredbydhi.help/2017/Coast_and_Sea/m3HD.pdf*, 2017.

[4] T. J. Thomas and G. Dwarakish. "numerical wave modelling - a review. *INTERNATIONAL CONFERENCE ON WATER RESOURCES, COASTAL AND OCEAN ENGINEERING (ICWRCOE'15)*, 4(443 - 448), 2015.